Accepted Manuscript

Lung inflammation does not affect the clearance kinetics of lipid nanocapsules following pulmonary administration

Aateka Patel, A. Woods, Yanira Riffo-Vasquez, Anna Babin-Morgan, Marie-Christine Jones, Stuart Jones, Kavitha Sunassee, Stephen Clark, Rafael Torres Martin de Rosales, Clive Page, Domenico Spina, Ben Forbes, Lea Ann Dailey

Please cite this article as: Aateka Patel, A. Woods, Yanira Riffo-Vasquez, Anna Babin-Morgan, Marie-Christine Jones, Stuart Jones, Kavitha Sunassee, Stephen Clark, Rafael Torres Martin de Rosales, Clive Page, Domenico Spina, Ben Forbes, Lea Ann Dailey, Lung inflammation does not affect the clearance kinetics of lipid nanocapsules following pulmonary administration, *Journal of Controlled Release* (2016), doi: 10.1016/j.jconrel.2016.05.024

Lung inflammation does not affect the clearance kinetics of lipid nanocapsules following pulmonary administration

Aateka Patel [a,b], A. Woods [b], Yanira Riffo-Vasquez [a], Anna Babin-Morgan [a,b], Marie-Christine Jones [c], Stuart Jones [b], Kavitha Sunassee [d], Stephen Clark [d], Rafael Torres Martin de Rosales [d], Clive Page [a,b], Domenico Spina [a, *] Ben Forbes [b#], Lea Ann Dailey [b,#,]

[a] Sackler Institute of Pulmonary Pharmacology, Institute of Pharmaceutical Science. King's College London, 150 Stamford Street, London SE1 9NH London, UK
[b] Drug Delivery Research Group, Institute of Pharmaceutical Science, King's College London, 150 Stamford Street, London SE1 9NH, UK
[c] University of Birmingham, Department of Pharmacy, Birmingham B15 2TT, UK
[d] Division of Imaging Sciences & Biomedical Engineering, King's College London, 4th Floor Lambeth Wing, St. Thomas' Hospital, SE1 7EH, London, UK.

* Corresponding author: Domenico Spina, email: domenico.spina@kcl.ac.uk; Telephone: +44 207 848 4341
[#] Joint senior authors for this study

ABSTRACT

Lipid nanocapsules (LNCs) are semi-rigid spherical capsules with a triglyceride core that present a promising formulation option for the pulmonary delivery of drugs with poor aqueous solubility. Whilst the biodistribution of LNCs of different size has been studied following intravenous administration, the fate of LNCs following pulmonary delivery has not been reported. We investigated quantitatively whether lung inflammation affects the clearance of 50 nm lipid nanocapsules, or is exacerbated by their pulmonary administration. Studies were conducted in mice with lipopolysaccharide-induced lung inflammation compared to healthy controls. Particle deposition and nanocapsule clearance kinetics were measured by single photon emission computed tomography/computed tomography (SPECT/CT) imaging over 48 h. A significantly lower lung dose of ^{111}In-LNC50 was achieved in the lipopolysaccharide (LPS)-treated animals compared with healthy controls (p < 0.001). When normalised to the delivered lung dose, the clearance kinetics of ^{111}In-LNC50 from the lungs fit a first order model with an elimination half-life of 10.5 ± 0.9 h (R^2 = 0.995) and 10.6 ± 0.3 h (R^2 = 1.000) for healthy and inflamed lungs respectively (*n* = 3). In contrast, ^{111}In-diethylene triamine pentaacetic acid (DTPA), a small hydrophilic molecule, was cleared rapidly from the lungs with the majority of the dose absorbed within 20 min of administration. Biodistribution to lungs, stomach-intestine, liver, trachea-throat and blood at the end of the imaging period was unaltered by lung inflammation. This study demonstrated that lung clearance and whole body distribution of lipid nanocapsules were unaffected by the presence of acute lung inflammation.

Keywords (maximum of 6): Lipid nanocapsules; pulmonary drug delivery; biodistribution; SPECT/CT; lung clearance kinetics; inflammation.

1. Introduction

A large proportion of compounds under development for inhaled therapy of respiratory disease have poor aqueous solubility or a short half-life in the lungs [1–3]. The aerosol administration of relatively insoluble compounds can result in a dose-dependent, solubility-dependent accumulation of particulate drug material in the lungs [4]. The long-term implications of macrophage responses to drugs of this nature is not completely understood and can be a barrier to the progress of such compounds to clinical development [5]. There are a variety of formulation strategies that may help circumvent the issues of insoluble particle accumulation in the airways, including the loading of agents in lipid nanocapsules [6].

Lipid nanocapsules are core-shell nanoparticle systems with an oily core comprised of triglycerides, a lipophilic material capable of dissolving compounds with poor aqueous solubility (e.g. the anti-cancer agents, paclitaxel and tretinoin) [7–10]. The core is surrounded by a semi-rigid shell typically consisting of phosphotidylcholines and surfactants [11]. Lipid nanocapsules can be manufactured on an industrial scale, exhibit long storage shelf-lives in suspension, demonstrate a high stability during nebulisation [9,12] and achieve constant, reproducible drug release profiles [13,14]. Furthermore, lipid nanocapsules have shown an excellent *in vivo* biocompatibility profile following single pulmonary administration across a range of therapeutically relevant doses [15,16] and are not associated with acute adverse macrophage responses [15].

While whole body distribution studies have been performed with lipid nanocapsules of different sizes following intravenous (i.v.) administration [17], the clearance and biodistribution of lipid nanocapsules following administration to the lungs has not been reported. Since lipid nanocapsules may be developed as drug carrier systems for the treatment of lung conditions which are likely to be accompanied by inflammation (e.g. respiratory infections, asthma or chronic obstructive pulmonary disease), it is important to study their biodistribution and clearance kinetics in the inflamed lung as well as healthy controls. Alternatively, if inhaled lipid nanocapsules were used as treatment vehicles in clinical scenarios where little or no lung inflammation was present (e.g. pulmonary hypertension or systemic delivery of drugs), it would be of relevance to understand whether the inhaled therapy would be affected by secondary respiratory tract infections [18,19]. Therefore, the aim of this study was to investigate the kinetics of lipid nanocapsule lung clearance and whole body distribution following administration to the mouse lung in the presence and absence of bacterial lipopolysaccharide (LPS), an endotoxin from Escherichia coli that induces acute lung inflammation [20–23]. It was hypothesised that (i) lipid nanocapsule administration to the inflamed lung would result in a modified clearance rate of the nanoformulation from the lungs compared to healthy control animals, but (ii) due to their high biocompatibility, lipid nanocapsules would not exacerbate the inflammation caused by the LPS pre-treatment.

2. Materials and Methods

2.1. Lipid nanocapsule manufacture and characterisation

Lipid nanocapsules were manufactured using the phase-inversion temperature method [11]. Briefly, lipid nanocapsules were prepared by generating a coarse emulsion of 17% w/w Labrafac®

Lipophile WL1349 (Gattefosse, Saint-Priest, France), 17.5% w/w Solutol® HS15 (BASF, Ludwigshafen, Germany), and 1.75% w/w Lipoid® S75-3 (Lipoid GmbH, Ludwigshafen, Germany) in a 3% w/w sodium chloride ($NaCl_{aq}$) solution. The emulsion was subjected to repeated heating and cooling cycles (85°-60°-85°-60°-85°C) before cooling to 72°C, quenching in a 2-fold volume of ice water and stirring at room temperature for 5-10 min. The nanocapsule suspension was filtered (0.45 μm syringe filter) and excess stabiliser (Solutol® HS15) was removed by dialysis (72 h) against water containing BioBeads® (BioRad, Hertfordshire, UK). Suspensions were concentrated prior to administration using ultrafiltration centrifuge tubes (Millipore Ltd., Hertfordshire, UK; 100 kDa MWCO). Residual Solutol® HS 15 content was < 0.5 mg/mL. Particle size and zeta potential were measured using a Zetasizer Nano ZS (Malvern, Worcestershire, UK). Nanocapsules were diluted 1:50 in purified water or saline and measurements taken at 25°C for quality control, at a scattering angle of 173°, using a viscosity value of water (0.8872 cP) for the dispersant. While all nanocapsule suspensions were size-stable for over four weeks when stored in purified water at 4°C [16], fresh batches were prepared for each *in vivo* experiment and used within 7 days of manufacture. Zeta potential measurements were performed at 25°C at a concentration of 20 μg/mL with all suspensions diluted in 6.3 mM $NaCl_{aq}$. Suspension concentration was determined gravimetrically.

2.2. Nanocapsule radiolabeling with [111]indium-chloride and stability studies

To incorporate a radiolabel chelator into the shell of the nanocapsule systems (radiolabeled formulation have been abbreviated as ^{111}In-LNC50), 0.1% w/w 1,2-dimyristoyl-sn-glycero-3-phosphoethanolamine-N-diethylenetriaminepentaacetic acid (DMPE-DTPA) (Avanti Polar Lipids Inc, Alabama, USA) was added to the components during the coarse emulsion step and the nanocapsules were prepared as described above. Suspensions were diluted to 12 mg/mL with 0.1 M ammonium acetate (pH 6.6) [24]. [111]Indium-chloride (Mallinckrodt Medical Inc, Petten, The Netherlands), ~50 MBq ([111]InCl_3, half-life 2.83 days), was dissolved in 0.5 M ammonium acetate (pH 5.0) and mixed with LNC50-DMPE-DTPA at a ratio of 1:2 v/v. The mixture was incubated at 37°C for 45 min under gentle shaking. Radiolabeling efficiency was measured by quantifying the radioactivity in the ultrafiltrate of the washing solution and washed particle residue after three cycles of washing using spin filtration with Amicon ultrafiltration centrifuge tubes (Millipore Ltd., Hertfordshire, UK; 30 kDa MWCO).

To assess the radiolabel stability in a biological environment, 5 μL of ^{111}In-LNC50 nanosuspensions (0.1-0.2 mg/mL) were added to 495 μL foetal bovine serum (FBS, Gibco (R), Life Technologies, UK) or phosphate buffered saline (PBS, pH 7.4; Oxiod Ltd, Basingstoke, UK) and incubated at 37°C with gentle shaking. At 24 and 48 h, ^{111}In-LNC50 were collected and centrifuged for 3 min at 10,000 g using ultrafiltration centrifuge tubes (30 kDa MWCO). The free ^{111}In content in the ultrafiltrate and particle residue was assayed using a Capintec/Mucha gamma counter (1282 Compugamma Laboratory Gamma Counter, LKB Wallac, Australia). For control experiments, diethylene triamine pentaacetic acid (DTPA) (Sigma-Aldrich, Dorset, UK) was dissolved in 0.5 M ammonium acetate (pH 6.6) to prepare a 1 mg/mL solution. [111]InCl_3 (37 MBq) was mixed with 0.5 M ammonium acetate (pH 6.6) at a 1:1 v/v ratio resulting in a final pH of 5.0. The ^{111}In solution (40 μL) was mixed with the DTPA solution (20 μL) and incubated at 37°C for 90 min to obtain ^{111}In-DTPA.

4

2.3. Induction of inflammation and administration of lipid nanocapsules

All procedures were conducted in accordance with the United Kingdom Animal Scientific Procedures Act, 1986 and were approved by the ethics committee of Kings College, London. *In vivo* experiments were performed with male BALB/C mice (6-8 weeks of age; Harlan, UK). Mice were housed in rooms maintained at a constant temperature (21 ± 2°C) and humidity (55 ± 15%) with a 12 h light-dark cycle. Animals had food and water available *ad libitum* and were allowed a 1 week acclimatisation period before use.

Animals were separated into six cohorts (*n* = 3-7) and were anaesthetised with isoflurane 3-5% v/v in O_2 at a flow rate of 1.0 L/min before intranasal (i.n.) administration of 25 µL of LPS (Sigma-Aldrich, Dorset, UK; 1 or 10 µg/mouse) or 0.9% saline (SAL; vehicle control for healthy animals). At t = 0 h, 25 µL of lipid nanocapsule suspension (175 µg/mouse) or saline vehicle control was administered using an oropharyngeal aspiration (o.a.) procedure [25]. Aspiration was confirmed visually.

2.4. Measurement of inflammation

Mice were killed humanely at 24 h with an intraperitoneal (i.p.) injection (0.5 mL) of 25% urethane. Lungs were lavaged with 3 x 0.5 mL of sterile 0.9% saline, which were combined and stored on ice. The lungs were removed and inflated with 10% formalin. Tissue histology was performed on three transverse sections cut through the left lung, dehydrated through ascending grades of ethanol and embedded in paraffin wax. Sections were stained with hematoxylin and eosin (H&E) stain to assess general morphology [26].

The total cell count in bronchoalveolar lavage (BAL) was determined immediately following lavage by mixing 50 µL BAL fluid with 50 µL Türk solution (Merck Chemicals, Darmstadt, Germany) and counting live cells using a haemocytometer. For differential cell counts, cytospin slides were prepared using 100 µL of BAL fluid spun at 1000 RCF for 1 minute. Slides were dried before differential staining (Reastain Quick-Diff Kit; Reagena Ltd, Toivala, Finland) and mounting (DPX; Fisher Scientific, Leicestershire, UK). A total of 100 cells were evaluated to determine the proportion of neutrophils, eosinophils and macrophages using standard morphological criteria. No eosinophils were detected in any of the samples. Total protein levels in BAL were quantified using a Quick Start™ Bradford Protein Assay (Bio-Rad, Hemel Hempstead, UK) according to manufacturer's instructions.

2.5. Single photon emission computed tomography/computed tomography (SPECT/CT) imaging

To measure clearance of lipid nanocapsules from healthy *versus* inflamed lungs, animals were grouped into four cohorts (*n* = 3). Intranasal pre-treatment with LPS (1 µg) or saline vehicle was performed as described above, followed 24 h later by o.a. administration of ^{111}In-LNC50 suspensions (125 µg solids/mouse, 2.5-3.0 MBq) or ^{111}In-DTPA (2.5-3.0 MBq) solutions. SPECT/CT scans were acquired for the whole body with mice placed in the prone position and a pressure transducer placed under the abdomen for respiratory monitoring. Scans were acquired at 0.25, 3, 24 and 48 h after [111]In- nanocapsule administration using a NanoSPECT/CT PLUS preclinical animal scanner (Mediso, Hungary). Mice dosed with ^{111}In-DTPA in PBS were treated as above with the exception of additional images collected at t = 0, 11, 23 and 35 min to capture the faster rate of clearance from the lungs (*n* = 1). CT images were obtained using a 55 kVP X-ray source, 500 ms

5

exposure time in 240 projections, a pitch of 1 and an acquisition time of 8 minutes. CT was imaged prior to SPECT, which was acquired using an exposure time of 1200 s, obtained over 60 projections and equipped with a 4-head scanner each with nine 1 mm pinhole apertures in helical scan mode with a total acquisition time of 35 min. CT images were reconstructed in a 352 × 352 matrix using proprietary Bioscan InVivSCope (Bioscan, USA) software, whereas SPECT images were reconstructed in a 256 × 256 matrix using HiSPECT (ScivisGmbH, Bioscan). Images were fused and analysed using InVivoScope (Version 1.44, Bioscan) for intensity counts. 3D regions of interests (ROI's) were created for desired organs at each time point using InviCRO 3D and the counts decay corrected and compared to the total delivered dose for each mouse to assess biodistribution and clearance. Following the final scan, mice were culled by cervical dislocation, tissue samples were excised, and radioactivity was counted in a gamma counter (LKB Wallac, Finland). The radiotracer activity in the samples was corrected for background decay time.

2.6. Organ distribution of lipid nanocapsules

A parallel set of animals were grouped into the same four cohorts (n = 3) to examine organ biodistribution. Inflammation was induced and ^{111}In-LNC50 or ^{111}In-DTPA were administered as described above. Mice were humanely killed with an i.p. injection of 0.5 mL urethane (25%) at 0.25, 3, 24 or 48 h after ^{111}In-LNC50 or ^{111}In-DTPA administration. Lungs were lavaged with 3 x 0.5 mL of sterile saline and a sample (200 μL) of BAL fluid was set aside whilst the remaining BAL was centrifuged for 20 min at 500 rpm to separate the supernatant from the cellular fraction. In addition, the throat, trachea, lungs, salivary glands, thymus, heart, stomach, intestines, liver, kidneys, spleen, bladder, faeces, muscle and blood were removed. Each sample was counted on a 1282 Compugamma Counter (LKB Wallac, Finland), together with standards prepared in a corresponding matrix. Data was corrected for radioactive decay during the experimental period and expressed as a percentage of the original activity.

2.7. Statistical analysis

Statistical Package for Social Sciences (SPSS) software (version 20.0; SPSS Inc., IBM, UK) was used for all statistical analyses. Data was analysed for normality using the Shapiro–Wilk test. Chelation stability was performed by systematic comparison of group means using a paired two-tailed Student's t-test. BAL cell counts from nanocapsule - and saline-challenged mice were compared using one way ANOVA on log transformed data followed by a post-hoc Tukey test. Particle size, lung clearance rates and 3-D image analysis from SPECT/CT was performed using a two way repeated measures ANOVA comparison with a post-hoc Bonferroni test. $p < 0.05$ was considered significant.

3. Results

3.1. Particle size, radiolabeling efficiency and stability of nanosuspensions

The lipid nanocapsules possessed a similar particle size, polydispersity index and surface charge to previously manufactured systems using similar conditions (Table 1) [11,15]. Incorporation of the chelator, DMPE-DTPA, into the shell of the nanocapsules resulted in marginally larger hydrodynamic diameters ($p < 0.01$) and an anionic surface charge (table 1) ($p < 0.01$). There was no significant change in the anionic surface charge between nanocapsules and

LNC50-DMPE-DTPA in 150 mM sodium chloride solution (p > 0.05). All systems were highly stable in suspension over a four week storage period (Supplementary Fig. S1). The surface charge of the labelled particles most probably arose as a consequence of the ionised carboxylic acid groups of DMPE-DTPA and it was suspected that this would probably be reduced once the $^{111}InCl_3$ was attached to the DMPE-DTPA. As a consequence the negative surface charge was not considered to have a significant impact on the surface chemistry of the particles when compared to the unlabelled material.

Table 1. *Particle size and surface charge of lipid nanocapsules with and without DMPE-DTPA incorporation. Data represents mean ± standard deviation of the hydrodynamic diameter (D_h), polydispersity index (PDI) and zeta potential of three batches of nanosuspensions in purified water, physiological saline (NaCl 150 mM) and a dilute saline solution (NaCl 6.3 mM) at 25°C.*

	Purified Water			NaCl (150 mM)			NaCl (6.3 mM)		
	D_h (nm)	PDI	ζ (mV)	D_h (nm)	PDI	ζ (mV)	D_h (nm)	PDI	ζ (mV)
Lipid nanocapsules (LNC50)	46.9 ± 0.4	0.1± 0.01	-7.7 ± 1.2	42.6 ± 0.2	0.05 ± 0.01	-2.6 ± 0.4	48.2 ± 0.4	0.05 ± 0.01	-4.7 ± 0.9
LNC50-DMPE-DTPA	50.7± 2.2	0.05 ± 0.03	-27.4 ± 3.5	46.7± 1.3	0.10 ± 0.01	-5.4 ± 1.2	52.7± 1.4	0.04 ± 0.02	-12.1 ± 2.3

The labelling efficiency of ^{111}In- nanocapsules (^{111}In-LNC50) was 91.2 ± 2.2 % (*n* = 5) when the filter binding of the label (6.8 ± 0.9 %) was accounted for and the ^{111}In-LNC50 were shown to be completely absent from the unbound label. This was demonstrated by a 98.0 ± 2.8 % (*n* = 5) recovery of the label during the washing process and the absence of significant levels of ^{111}In in the ultrafiltrate of suspensions following incubation in FBS and PBS (150 mM, pH 7.4) (*n* = 3; p > 0.05).

3.2. Lung inflammation

LPS was used to induce airway neutrophilia to determine whether nanocapsule administration to inflamed lungs exacerbates the pre-existing inflammation. Administration of LPS (10 and 1 µg i.n.) was used to induce a robust acute inflammatory response in the mouse lung characterised by an increase in total BAL cell numbers and a significant increase in BAL neutrophils (Fig. 1B-C). The 10 µg dose represented a typical LPS model of neutrophilic inflammation and it was observed that LNC administration did not exacerbate the inflammation. It was not possible to use the higher LPS dose in imaging studies, as animals with a moderate level of lung inflammation were susceptible to respiratory distress under the prolonged anaesthesia necessary for image acquisition. Therefore, a 1 µg dose of LPS was used to induce a mild, but significant, inflammatory response which was also not influenced by LNC administration. In all LPS-treated cohorts, the neutrophilic response was fully resolved by t = 72 h post-administration of LPS (data not shown).

Lipid nanocapsule treatment using an o.a. procedure did not induce acute inflammation in healthy lungs (Fig. 1B-D), thus confirming previous findings [15,16]. Histological analysis of lung tissue showed an accumulation of neutrophils in the lungs obtained from mice pre-treated with LPS (Fig. 2C-D) in comparison to mice with a saline pre-treatment (Fig. 2A-B). LPS-induced inflammation was characterised by peri- bronchial foci of neutrophils and fibrin, prominence of alveolar macrophages, and intra-alveolar haemorrhage. No significant differences in BAL total protein could be detected between the treatment groups ($p > 0.05$). BAL fluid cytokine analysis was not performed in this study, as we have previously published cytokine levels post-LNC administration [15].
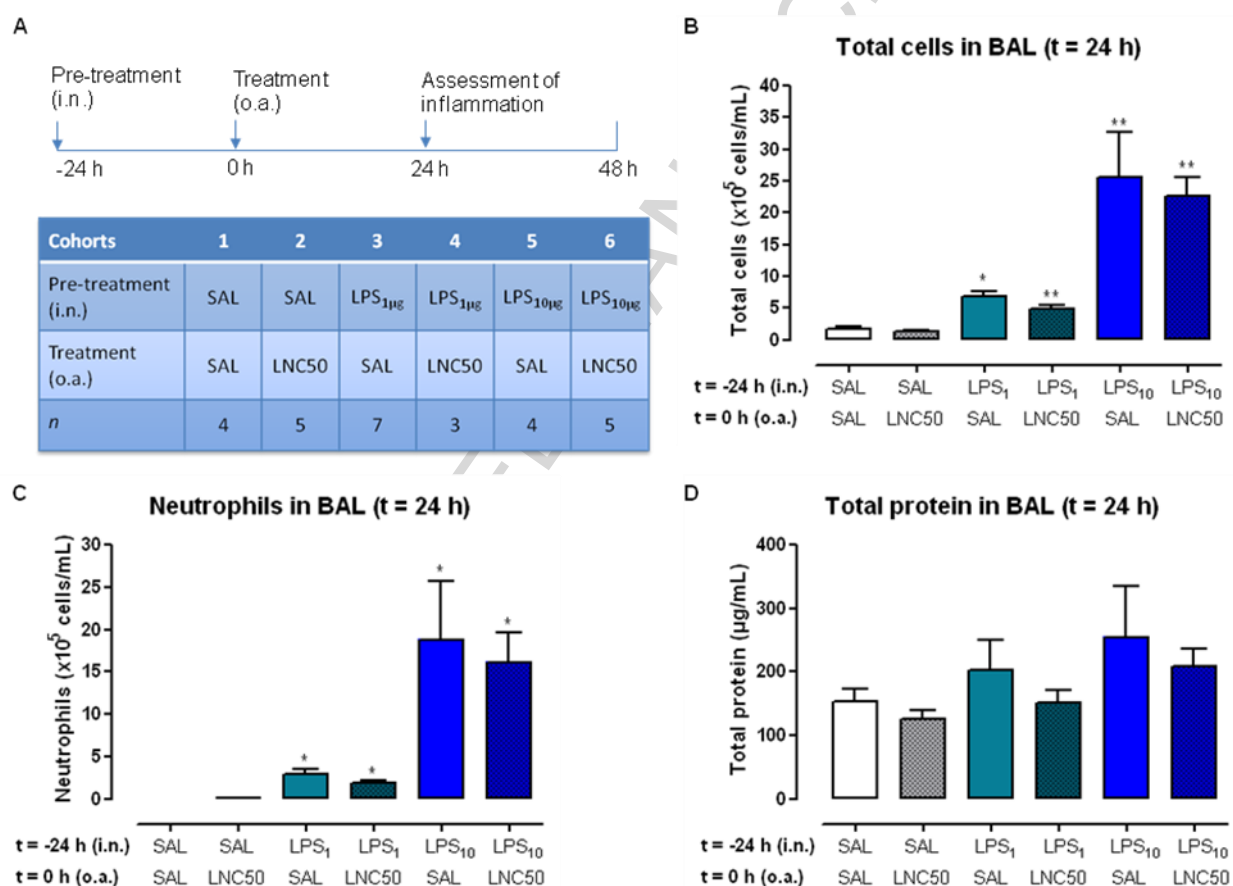

Fig. 1. *Assessment of inflammatory parameters in bronchoalveolar lavage (BAL). (A) dosing schedule, (B) total number of cells, (C) neutrophils and (D) total protein in BAL at t = 24 h into the dosing schedule. Columns represent mean ± SEM (n = 3-7). No significant difference between the (SAL)/SAL (saline control) and (SAL)/LNC50 (treatment) groups was observed. LPS pre-treatment increased inflammatory parameters compared with the respective saline control; * p < 0.05, ** p < 0.01.*
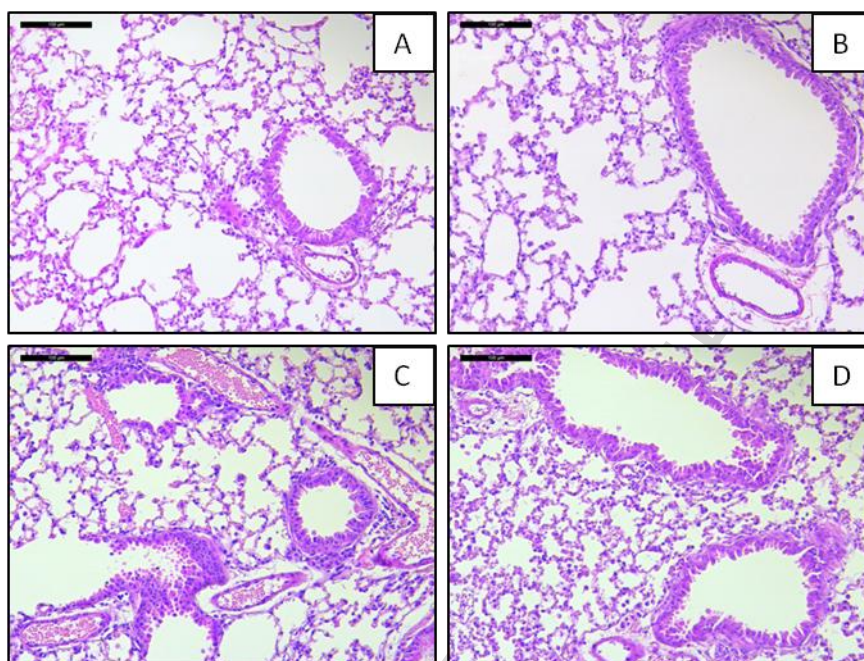
Fig. 2. Histopathology of lung tissue exposed to lipid nanocapsules following saline or LPS pre-treatment. Representative images of lung tissue harvested at t = 48 h from the following treatment groups: A) (SAL)/SAL, B) (SAL)/ LNC50, C) (LPS)/SAL, or D) (LPS)/LNC50 (20× magnification; scale bar = 100 μm).

3.3. Lung clearance and biodistribution using non-invasive longitudinal SPECT/CT imaging

Four cohorts of animals (Fig. 3A) were used to investigate whether lung clearance and subsequent biodistribution of ^{111}In-LNC50 was influenced by lung inflammation. The small, hydrophilic molecule, ^{111}In-DTPA, was used as a control for ligand-radiolabel stability in the nanocapsules. As expected, ^{111}In-DTPA lung clearance was extremely rapid, with a majority of the o.a. administered dose crossing the air-blood barrier within the first 25 min post-administration (Fig. 3B) and a majority of the signal accumulating in the kidneys and bladder [27,28], from where it was eliminated within 24 h (Fig. 3C-D). No detectable differences in ^{111}In-DTPA lung clearance were observed between the healthy *versus* inflamed lung (Fig. 3C-D). SPECT/CT images of o.a.-administered ^{111}In-LNC50 revealed that lipid nanocapsules were cleared from the lungs over 48 h. Analysis of the signal in the mouth, trachea and lungs at the first image acquisition time showed that a lower lung dose (total activity/organ) was observed in the (LPS$_{1\mu g}$)/^{111}In-LNC50-treated animals compared with saline (SAL)/^{111}In-LNC50 treated animals. No qualitative differences in ^{111}In-LNC50 lung clearance were observed between the healthy *versus* inflamed lungs (Fig. 3E-F).
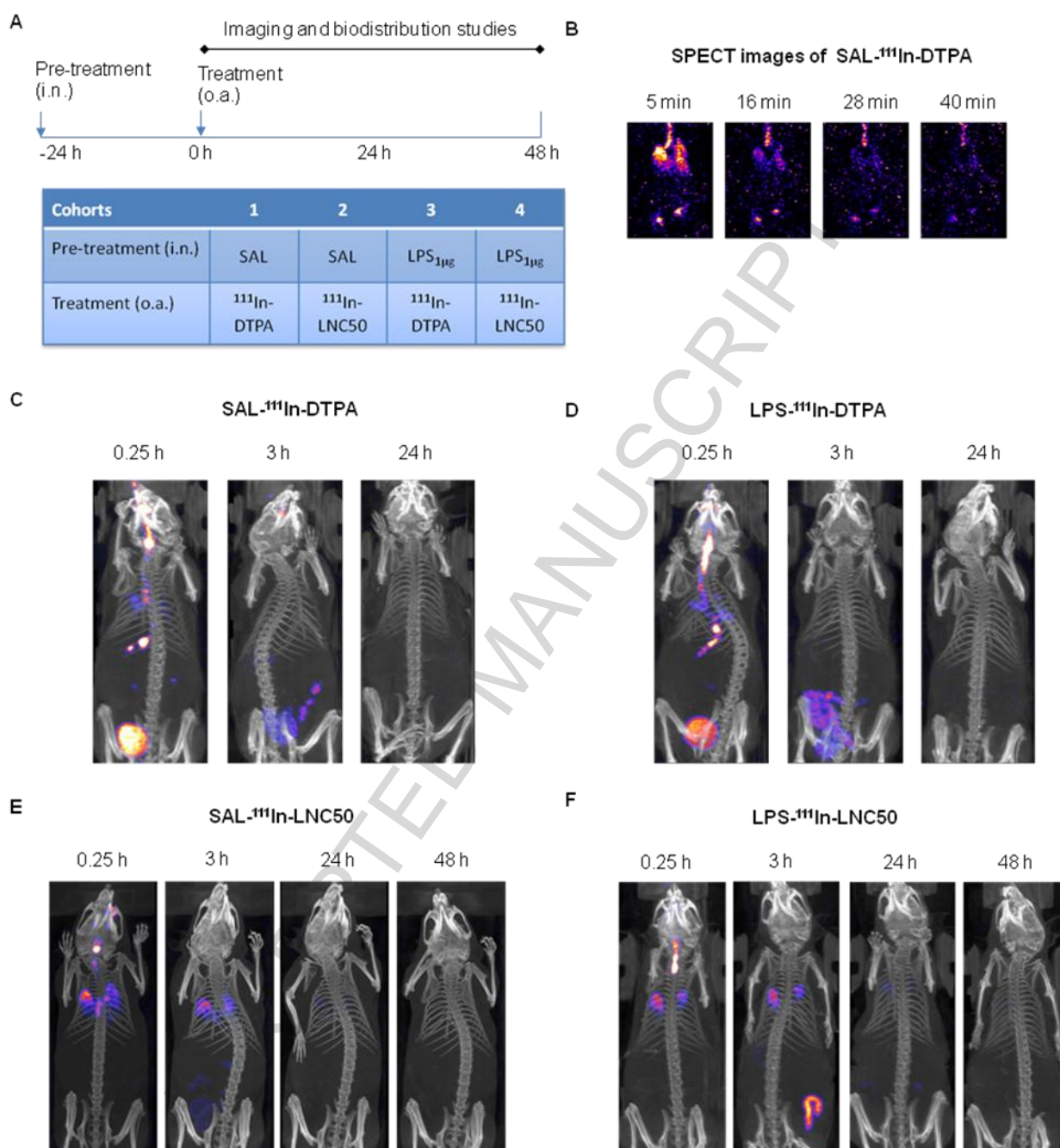
Fig. 3. Whole-body SPECT/CT images of ^{111}In-DTPA or ^{111}In-LNC50 following pre-treatment with LPS (1 μg) or saline (SAL). A) Dosing schedule. B) Rapid acquisition of a sequence of SPECT images of the mouse thorax at t = 5, 15, 25, and 35 min post ^{111}In-DTPA administration (o.a.) was necessary to monitor the clearance of ^{111}In-DTPA from the lungs. SPECT/CT images of the whole body were acquired over 24 h for (SAL)/^{111}In-DTPA (C) and (LPS$_{1μg}$)/^{111}In-DTPA (D) treatment groups, while (SAL)/^{111}In-LNC50 (E) and (LPS$_{1μg}$)/^{111}In-LNC50 (F) treatment groups were monitored from up to 48 h. All activity has been decay corrected and compared against the first scan at 0.25 h (i.e. 15 min post o.a. administration) for each mouse.

3-D image analysis was used to study the biodistribution of the radiolabelled systems semi-quantitatively for 48 h post-administration. The lungs, intestines, bladder and liver, were chosen

as regions of interest for quantitative analysis (Fig. 4). The lung dose of the ^{111}In-LNC50 was significantly higher at the first scan (0.25 h post-dosing) compared to ^{111}In-DTPA (p < 0.001), because ^{111}In-DTPA rapidly crossed the air-blood barrier rapidly into the systemic circulation and accumulated in the bladder (Fig. 3B, 4A, C). A statistically significant, lower lung dose (total activity/organ) was observed in the (LPS$_{1\mu g}$)/^{111}In-LNC50 treated animals (35.08 ± 5.27%) at 0.25 h compared with (SAL)/^{111}In-LNC50 treated animals (51.63 ± 3.29%) (Fig. 4A; p < 0.001). Analysis of the signal in the mouth, trachea and lungs at the first image acquisition time (t = 0.25 h) revealed that LPS-treated animals typically showed a lower lung and higher mouth signal distribution, whereas the pattern was reversed in healthy mice (Fig. 4E), which may indicate that animals with lung inflammation had a lower inspiratory capacity and did not aspirate liquid into the lungs to the same extent as their healthy counterparts. Notably, only ^{111}In-LNC50- treated animals showed an accumulation of signal in the liver, peaking at t = 24 h, possibly indicating that a portion of the nanocapsule dose were able to traverse the air-blood barrier and enter the systemic circulation intact, whereby they encountered circulating phagocytic cells in the blood and were cleared to the liver [29,30].
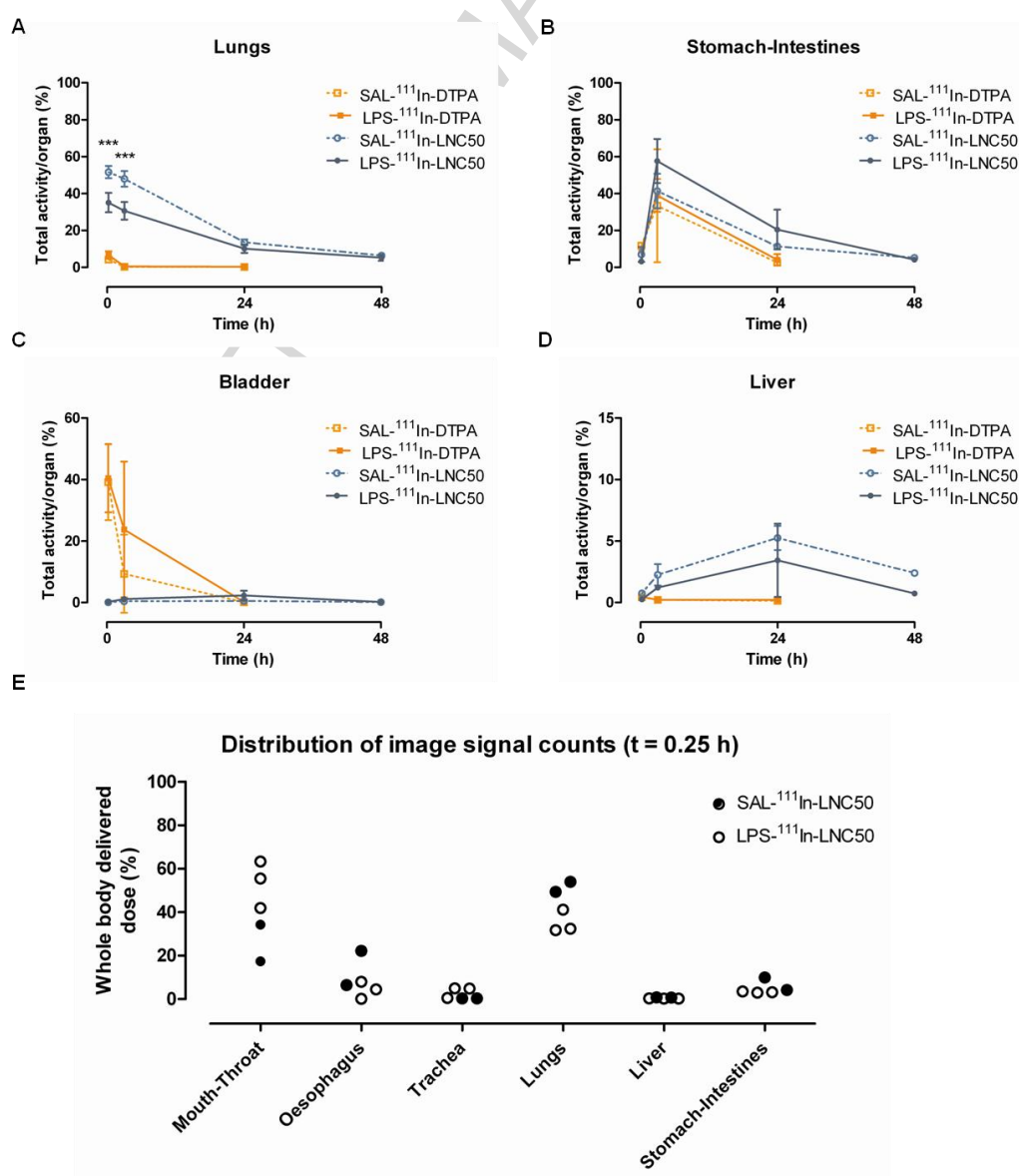
Fig. 4. *Distribution of ^{111}In-DTPA and ^{111}In-LNC50 nanosuspensions administered by oral aspiration to mice with the healthy vs. inflamed lungs. The ^{111}In signal per organ was measured by 3-D image analysis over 48 h and is reported as a percentage of the total signal count from the first acquired image (with correction for signal decay). Signal distribution is reported for the (A) lungs, (B) stomach-intestines, (C) bladder and (D) liver. Values represent the mean ± standard deviation from n = 3 animals in each cohort (n=2 for the (SAL)/^{111}In-LNC50 group, due to exclusion of one mouse where the majority of the dose was ingested). (E) Signal distribution of ^{111}In-LNC50 in various organs of individual animals in the first full SPECT/CT image (t = 0.25 h of the study schedule) is shown to evaluate whether the LPS model of inflammation affects the pulmonary dose following o.a. administration. (***) p < 0.001, statistically significant between (SAL)/^{111}In-LNC50 vs. (LPS$_{1\mu g}$)/^{111}In-LNC50.*

The lung clearance kinetics of ^{111}In-DTPA and ^{111}In-LNC50 suspensions were calculated from the imaging data after normalisation to the original lung dose. The clearance kinetics of ^{111}In-LNC50 from the lungs fit a first order model (Fig. 5) with an elimination half-life of 10.5 ± 0.9 h (R^2 = 0.9950) and 10.6 ± 0.3 h (R^2 = 0.9996) for groups pre-treated with saline and LPS$_{1\mu g}$, respectively (p > 0.05).
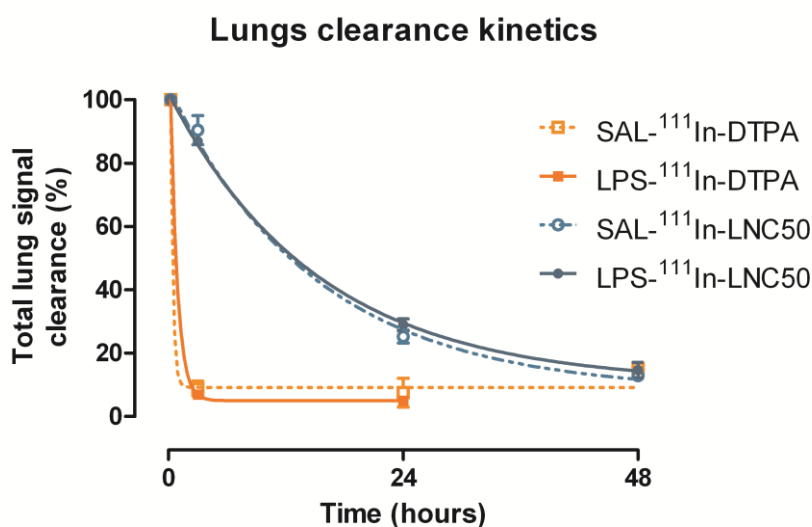

Fig. 5. *Lung clearance kinetics from SPECT/CT images for ^{111}In-DTPA and ^{111}In-LNC50 in mice with healthy vs. inflamed lungs (n = 3). Values have been corrected for decay and normalised to the initially deposited lung dose for lung clearance. Curves for ^{111}In-LNC50 were fitted according to a one phase exponential decay model (Prism 5.0, Graphpad). p > 0.05, (SAL)/^{111}In-LNC50 vs. (LPS$_{1\mu g}$)/^{111}In-LNC50.*

3.4. Lung clearance and biodistribution using terminal end-point studies

Nanocapsule distribution and clearance from the lungs, was evaluated further using terminal end-point studies with the same dosing schedules as the imaging studies (Fig. 6A-H; Supplementary Information Fig. S2A-H). The biodistribution profiles from terminal end-point studies were very similar to the SPECT/CT profiles demonstrating that non-invasive, longitudinal imaging is a reliable and useful alternative methodology. Only minor differences between the two methods were observed. For instance, sequential SPECT scanning was better suited to assess the rapid clearance of compounds, such as ^{111}In-DTPA from the lungs, compared to end-point studies. However, SPECT imaging was not able to detect the diluted radiolabel signals present in the bloodstream; for this application, blood sampling and γ-scintigraphy measurement was required.

12

The localisation of the radioactive signal within the lungs over time was assessed by lung lavage performed at t = 3 and 24 h per treatment group with the radioactivity measured in the total BAL (i.e. BAL fluid + cellular fraction) as well as the isolated BAL cellular fraction. The radioactivity recovered in the BAL generally reflected the lung clearance profiles of the respective systems. ^{111}In-DTPA was observed primarily in the BAL fluid and was cleared within the first 25 min after dosing, while ^{111}In-nanosuspensions remained in the total BAL fluid and cleared slowly.

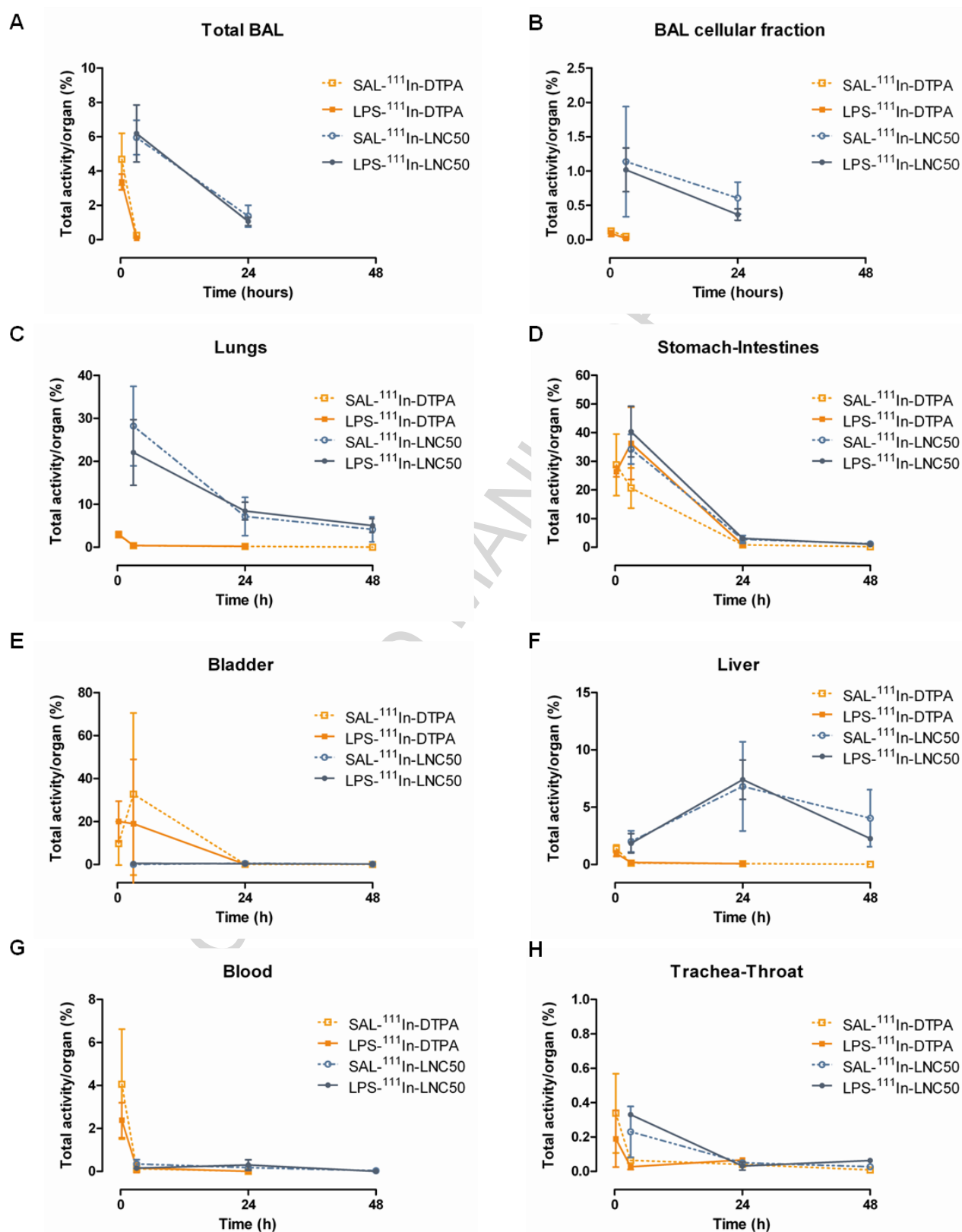**Fig. 6.** *Biodistribution of ^{111}In-DTPA and ^{111}In-LNC50 nanosuspensions after delivery by oral aspiration to mice with healthy vs. inflamed lungs. The distribution of radioactivity is reported in isolated fluids/organs after animal sacrifice for A) total BAL, B) BAL cellular fraction, C) lungs, D) stomach-intestines, E) bladder, F) liver, G) blood and H) trachea-throat. Values have been corrected for decay and represent the mean ± standard deviation from n = 3 animals at each time point.*

4. Discussion

Lipid nanocapsules are promising drug carriers systems for compounds such as those with poor aqueous solubility (e.g. paclitaxel and trerinoin) [7,10,31,32] and compounds benefitting from an extended retention time in the lungs (e.g. iloprost) [33]. Some of these compounds may be used to treat conditions that are accompanied by lung inflammation (e.g. asthma, COPD, respiratory tract infections), while in other therapeutic scenarios lung inflammation may not be a feature (e.g. pulmonary hypertension, lung cancer, systemic delivery of drugs). For indications where lung inflammation is not a prominent feature, it is important to determine whether any secondary inflammation acquired during the therapy (e.g. a lung infection) will influence the pharmacokinetic profiles of the inhaled compound. For example, several important clinical studies have been carried out to investigate whether upper respiratory tract infections influenced the pharmacokinetic profiles of inhaled insulin formulations [18,19]. To date, there are no published studies investigating whether inhaled nanoparticle drug carriers will positively or negatively influence an existing lung inflammation or alternatively whether the inflamed lung will influence the clearance profile and resulting pharmacokinetics of inhaled nanomedicines. Both are clinically relevant questions, which are addressed in the current study using lipid nanocapsules as an example of an advanced formulation strategy with real clinical potential.

Similar to previously published reports [15,16], lipid nanocapsule administration to the healthy lung was well tolerated. Importantly, nanocapsule administration to a murine model of neutrophilic airway inflammation did not to exacerbate the pre-existing inflammatory condition. Contrary to the study hypothesis, lipid nanocapsule clearance kinetics was not influenced by a pre-existing mild lung inflammation. It would be interesting to see whether a threshold of severity of lung inflammation exists above which an effect might be seen. This might be accomplished more readily with terminal end-point studies or imaging methods with faster acquisition times, both of which would not require prolonged periods of anaesthesia and would be more compatible with disease models of a higher severity.

Interestingly, nanocapsule lung clearance kinetics were more rapid than expected, with a half-life of ~10.5 h, in contrast to other nanocarriers reported in the literature, such as albumin nanoparticles (~200 nm; clearance half-life ~96 h) and albumin protein in solution (~4-6 nm) [34]. This profile indicates a moderate lung retention, which could be compatible with a once-a-day administration frequency and a sustained drug release profile over a 24 h period. Therapeutic applications for such a pharmacokinetic-modulating formulation include the treatment of pulmonary hypertension with inhaled iloprost (Ventavis®), which due to the short half-life of iloprost in the lung requires administration frequencies of 6-9 doses per day [35].

Both the imaging and terminal end-point biodistribution studies provided an indication of the fate of lipid nanocapsules following o.a. administration. In the lung, the nanocapsules remained primarily in the lung lining fluid avoiding phagocytosis by alveolar macrophages, a behaviour which was attributed to the pegylated ('stealth') surface chemistry and the small particle size, which reduce macrophage detection and phagocytosis [36–38], whilst promoting translocation across the air-blood barrier [29,30,39]. The increase in signal in the liver at t=24 h post-administration (absent in the ^{111}In-DTPA groups) suggests that at least a fraction of the lung dose was able to cross the air-blood barrier and enter into the systemic circulation as intact

15

nanoparticles, accumulating subsequently in the liver [29,30]. Previous studies have shown that lipid nanocapsules are highly stable in biological fluids, such as cell culture media and gastric fluids [40,41]; although nanocapsule stability and drug release studies have yet to be performed in lung lining fluid or lung lining fluid mimetics. *In vitro* studies have also shown that lipid nanocapsules are able to traverse epithelial cell monolayers intact, possibly through transcytosis [42], however, this may not be the only mechanism by which nanocapsules are cleared from the lung in vivo. Mucociliary clearance and subsequent swallowing may have also cleared a fraction of the lung dose especially that delivered to the upper airways, bronchi and trachea. When ^{111}In-DTPA or ^{111}In-LNC50 were administered by o.a., it was impossible to quantify mucociliary clearance from the imaging and terminal end-point studies as there were high GI tract signal levels in the first 24 h resulting from the swallowed fraction of the dose (~60%) at the point of administration. However, by 24 h the ingested dose was eliminated and signal levels in the GI tract from 24-48 h were nearly undetectable, indicating that mucociliary clearance was not a major pathway for lipid nanocapsule removal from the lungs after 24 h. Interestingly, no systemic absorption of ^{111}In-LNC50 components from the GI-tract was observed in animals where the majority of the entered the GI-tract instead of the lung (Supplementary Fig. S3A-E), which supports the observation that the liver accumulation measured in the current study resulted from the lung fraction, rather than the ingested fraction of the dose.

5. Conclusions

Few clinical trials and even fewer studies in animal models have investigated the effect of inflammation on the clearance of drugs or nanocarriers from the lungs. This study demonstrated that pulmonary delivery of lipid nanocapsules was well tolerated after a single dose and does not exacerbate an existing acute lung inflammation. Lipid nanocapsules exhibited clearance half-life of ~10.5 h regardless of whether the lung was healthy or inflamed. The safety and lung retention verifies that the nanocapsules are a promising option for modulating the pharmacokinetics of drugs delivered to the lungs. This study provides clinically relevant information that will be useful for guiding the design of future drug formulation studies with lipid nanocapsules as a drug carrier for a wide range of applications.

References

[1]   J.A. Tolman, R.O. Williams, Advances in the pulmonary delivery of poorly water-soluble drugs: influence of solubilization on pharmacokinetic properties, Drug Dev. Ind. Pharm. 36 (2010) 1–30. doi:10.3109/03639040903092319.

[2]   A.E. Cooper, D. Ferguson, K. Grime, Optimisation of DMPK by the Inhaled Route: Challenges and Approaches, Curr. Drug Metab. 13 (2012) 457–473. doi:10.2174/138920012800166571.

[3]   A.J. Hickey, Controlled delivery of inhaled therapeutic agents, J. Control. Release. 190 (2014) 182–188. doi:10.1016/j.jconrel.2014.05.058.

[4]   R.M. Jones, N. Neef, Interpretation and prediction of inhaled drug particle accumulation in the lung and its associated toxicity, Xenobiotica. 42 (2012) 86–93. doi:10.3109/00498254.2011.632827.

[5]   B. Forbes, R. O'Lone, P.P. Allen, A. Cahn, C. Clarke, M. Collinge, et al., Challenges for inhaled drug discovery and development: Induced alveolar macrophage responses, Adv. Drug Deliv. Rev. 71 (2014) 15–33. doi:10.1016/j.addr.2014.02.001.

[6]   C. Loira-Pastoriza, J. Todoroff, R. Vanbever, Delivery strategies for sustained drug release in the lungs, Adv. Drug Deliv. Rev. 75 (2014) 81–91. doi:10.1016/j.addr.2014.05.017.

[7]   F. Lacoeuille, E. Garcion, J.-P. Benoit, A. Lamprecht, Lipid nanocapsules for intracellular drug delivery of anticancer drugs., J. Nanosci. Nanotechnol. 7 (2007) 4612–4617. doi:10.1166/jnn.2007.006.

[8]   N.T. Huynh, C. Passirani, P. Saulnier, J.P. Benoit, Lipid nanocapsules: A new platform for nanomedicine, Int. J. Pharm. 379 (2009) 201–209. doi:10.1016/j.ijpharm.2009.04.026.

[9]   J. Hureaux, F. Lagarce, F. Gagnadoux, L. Vecellio, A. Clavreul, E. Roger, et al., Lipid nanocapsules: Ready-to-use nanovectors for the aerosol delivery of paclitaxel, Eur. J. Pharm. Biopharm. 73 (2009) 239–246. doi:10.1016/j.ejpb.2009.06.013.

[10]   E. Schultze, A. Ourique, V.C. Yurgel, K.R. Begnini, H. Thurow, P.M.M. De Leon, et al., Encapsulation in lipid-core nanocapsules overcomes lung cancer cell resistance to tretinoin, Eur. J. Pharm. Biopharm. 87 (2014) 55–63. doi:10.1016/j.ejpb.2014.02.003.

[11]   B. Heurtault, P. Saulnier, B. Pech, J.E. Proust, J.P. Benoit, A novel phase inversion-based process for the preparation of lipid nanocarriers, Pharm. Res. 19 (2002) 875–880. doi:10.1023/A:1016121319668.

[12]   A. Kumar, L.A. Dailey, B. Forbes, Lost in translation: what is stopping inhaled nanomedicines from realizing their potential?, Ther. Deliv. 5 (2014) 757–761. doi:10.4155/tde.14.47.

[13]   A. Lamprecht, Y. Bouligand, J.P. Benoit, New lipid nanocapsules exhibit sustained release properties for amiodarone, J. Control. Release. 84 (2002) 59–68. doi:10.1016/S0168-3659(02)00258-4.

[14]   M.M.A. Abdel-Mottaleb, D. Neumann, A. Lamprecht, In vitro drug release mechanism from lipid nanocapsules (LNC), Int. J. Pharm. 390 (2010) 208–213. doi:10.1016/j.ijpharm.2010.02.001.

[15]   M.C. Jones, S.A. Jones, Y. Riffo-Vasquez, D. Spina, E. Hoffman, A. Morgan, et al., Quantitative assessment of nanoparticle surface hydrophobicity and its influence on pulmonary biocompatibility, J. Control. Release. 183 (2014) 94–104. doi:10.1016/j.jconrel.2014.03.022.
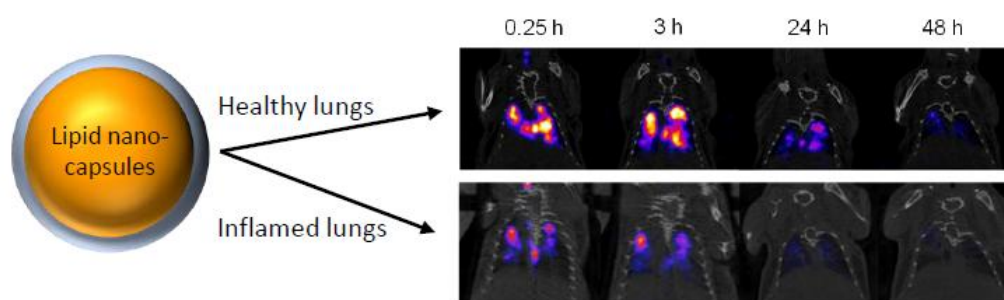
[16] L.A. Dailey, R. Hernández-Prieto, A.M. Casas-Ferreira, M.-C. Jones, Y. Riffo-Vasquez, E. Rodríguez-Gonzalo, et al., Adenosine monophosphate is elevated in the bronchoalveolar lavage fluid of mice with acute respiratory toxicity induced by nanoparticles with high surface hydrophobicity., Nanotoxicology. 5390 (2014) 1–10. doi:10.3109/17435390.2014.894150.

[17] S. Hirsjärvi, S. Dufort, J. Gravier, I. Texier, Q. Yan, J. Bibette, et al., Influence of size, surface coating and fine chemical composition on the in vitro reactivity and in vivo biodistribution of lipid nanocapsules versus lipid nanoemulsions in cancer models, Nanomedicine Nanotechnology, Biol. Med. 9 (2013) 375–387. doi:10.1016/j.nano.2012.08.005.

[18] A. McElduff, L.E. Mather, P.C. Kam, P. Clauson, Influence of acute upper respiratory tract infection on the absorption of inhaled insulin using the AERx?? insulin Diabetes Management System, Br. J. Clin. Pharmacol. 59 (2005) 546–551. doi:10.1111/j.1365-2125.2005.02366.x.

[19] J.E. Gern, C.K. Stone, M. Nakano, D.B. Muchmore, A. de la Peña, S. Park, et al., Effect of upper respiratory tract infection on AIR inhaled insulin pharmacokinetics and glucodynamics in healthy subjects., 2008. doi:10.1038/sj.clpt.6100286.

[20] R.J. Szarka, N. Wang, L. Gordon, P.N. Nation, R.H. Smith, A murine model of pulmonary damage induced by lipopolysaccharide via intranasal instillation., J. Immunol. Methods. 202 (1997) 49–57.

[21] K.N. Kornerup, G.P. Salmon, S.C. Pitchford, W.L. Liu, C.P. Page, Circulating platelet-neutrophil complexes are important for subsequent neutrophil activation and migration., J. Appl. Physiol. 109 (2010) 758–767. doi:10.1152/japplphysiol.01086.2009.

[22] H.F. Håkansson, A. Smailagic, C. Brunmark, A. Miller-Larsson, H. Lal, Altered lung function relates to inflammation in an acute LPS mouse model, Pulm. Pharmacol. Ther. 25 (2012) 399–406. doi:10.1016/j.pupt.2012.08.001.

[23] Y. Riffo-Vasquez, F. Man, C.P. Page, Doxofylline, a novofylline inhibits lung inflammation induced by lipopolysacharide in the mouse, Pulm. Pharmacol. Ther. 27 (2014) 170–178. doi:10.1016/j.pupt.2014.01.001.

[24] N. Mitchell, T.L. Kalber, M.S. Cooper, K. Sunassee, S.L. Chalker, K.P. Shaw, et al., Incorporation of paramagnetic, fluorescent and PET/SPECT contrast agents into liposomes for multimodal imaging, Biomaterials. 34 (2013) 1179–1192. doi:10.1016/j.biomaterials.2012.09.070.

[25] H.F. Lakatos, H. a Burgess, T.H. Thatcher, M.R. Redonnet, E. Hernady, J.P. Williams, et al., Oropharyngeal aspiration of a silica suspension produces a superior model of silicosis in the mouse when compared to intratracheal instillation, Exp. Lung Res. 32 (2006) 181–199. doi:10.1080/01902140600817465.

[26] C. Egger, C. Cannet, C. Gérard, E. Jarman, G. Jarai, A. Feige, et al., Administration of Bleomycin via the Oropharyngeal Aspiration Route Leads to Sustained Lung Fibrosis in Mice

and Rats as Quantified by UTE-MRI and Histology, PLoS One. 8 (2013) e63432. doi:10.1371/journal.pone.0063432.

[27] M.A. Videira, M.F. Botelho, A.C. Santos, L.F. Gouveia, J.J.P. de Lima, A.J. Almeida, Lymphatic uptake of pulmonary delivered radiolabelled solid lipid nanoparticles., J. Drug Target. 10 (2002) 607–613. doi:10.1080/1061186021000054933.

[28] C.G. Tankersley, J. a Shank, S.E. Flanders, S.E. Soutiere, R. Rabold, W. Mitzner, et al., Changes in lung permeability and lung mechanics accompany homeostatic instability in senescent mice., J. Appl. Physiol. 95 (2003) 1681–1687. doi:10.1152/japplphysiol.00190.2003.

[29] M. Semmler, J. Seitz, F. Erbe, P. Mayer, J. Heyder, G. Oberdörster, et al., Long-term clearance kinetics of inhaled ultrafine insoluble iridium particles from the rat lung, including transient translocation into secondary organs., Inhal. Toxicol. 16 (2004) 453–459. doi:10.1080/08958370490439650.

[30] W.G. Kreyling, S. Hirn, W. Möller, C. Schleh, A. Wenk, G. Celik, et al., Air-blood barrier translocation of tracheally instilled gold nanoparticles inversely depends on particle size, ACS Nano. 8 (2014) 222–233. doi:10.1021/nn403256v.

[31] S. Peltier, J.M. Oger, F. Lagarce, W. Couet, J.P. Benoît, Enhanced oral paclitaxel bioavailability after administration of paclitaxel-loaded lipid nanocapsules, Pharm. Res. 23 (2006) 1243–1250. doi:10.1007/s11095-006-0022-2.

[32] K.A. Shah, A.A. Date, M.D. Joshi, V.B. Patravale, Solid lipid nanoparticles (SLN) of tretinoin: Potential in topical delivery, Int. J. Pharm. 345 (2007) 163–171. doi:10.1016/j.ijpharm.2007.05.061.

[33] P. Jain, G. Leitinger, R. Leber, C. Nagaraj, B. Lehofer, H. Olschewski, et al., Liposomal nanoparticles encapsulating iloprost exhibit enhanced vasodilation in pulmonary arteries, Int. J. Nanomedicine. (2014) 3249. doi:10.2147/IJN.S63190.

[34] A. Woods, A. Patel, D. Spina, Y. Riffo-Vasquez, A. Babin-Morgan, R.T.M. de Rosales, et al., In vivo biocompatibility, clearance, and biodistribution of albumin vehicles for pulmonary drug delivery, J. Control. Release. 210 (2015) 1–9. doi:10.1016/j.jconrel.2015.05.269.

[35] B. Vaidya, V. Gupta, Novel therapeutic approaches for pulmonary arterial hypertension: Unique molecular targets to site-specific drug delivery., J. Control. Release. 211 (2015) 118–133. doi:10.1016/j.jconrel.2015.05.287.

[36] I.M. Rio-Echevarria, F. Selvestrel, D. Segat, G. Guarino, R. Tavano, V. Causin, et al., Highly PEGylated silica nanoparticles: 'ready to use' stealth functional nanocarriers, J. Mater. Chem. 20 (2010) 2780. doi:10.1039/b921735e.

[37] J.L. Perry, K.G. Reuter, M.P. Kai, K.P. Herlihy, S.W. Jones, J.C. Luft, et al., PEGylated PRINT nanoparticles: The impact of PEG density on protein binding, macrophage association, biodistribution, and pharmacokinetics, Nano Lett. 12 (2012) 5304–5310. doi:10.1021/nl302638g.

[38]   S. Salmaso, P. Caliceti, Stealth properties to improve therapeutic efficacy of drug nanocarriers., J. Drug Deliv. 2013 (2013) 374252. doi:10.1155/2013/374252.

[39]   M. Semmler-Behnke, W.G. Kreyling, J. Lipka, S. Fertsch, A. Wenk, S. Takenaka, et al., Biodistribution of 1.4- and 18-nm gold particles in rats, Small. 4 (2008) 2108–2111. doi:10.1002/smll.200800922.

[40]   E. Roger, F. Lagarce, J.P. Benoit, The gastrointestinal stability of lipid nanocapsules, Int. J. Pharm. 379 (2009) 260–265. doi:10.1016/j.ijpharm.2009.05.069.

[41]   J. Chana, B. Forbes, S.A. Jones, Triggered-release nanocapsules for drug delivery to the lungs, Nanomedicine Nanotechnology, Biol. Med. 11 (2015) 89–97. doi:10.1016/j.nano.2014.07.012.

[42]   E. Roger, F. Lagarce, E. Garcion, J.P. Benoit, Lipid nanocarriers improve paclitaxel transport throughout human intestinal epithelial cells by using vesicle-mediated transcytosis, J. Control. Release. 140 (2009) 174–181. doi:10.1016/j.jconrel.2009.08.010.

*Graphical Abstract